

2010

Influences on the prediction of conveyor trajectory profiles

David B. Hastie

University of Wollongong, dhastie@uow.edu.au

P W. Wypych

University of Wollongong, peter_wypych@uow.edu.au

P C. Arnold

University of Wollongong, peter_arnold@uow.edu.au

Publication Details

Hastie, DB, Wypych, PW & Arnold, PC, Influences on the prediction of conveyor trajectory profiles, *Particulate Science and Technology*, 28(2), 2010, p 132-145.

Influences on the Prediction of Conveyor Trajectory Profiles

D.B. Hastie*
P.W. Wypych
P.C. Arnold

Centre for Bulk Solids and Particulate Technologies
Faculty of Engineering, University of Wollongong
Wollongong, New South Wales, Australia

*Address correspondence to David Hastie, Centre for Bulk Solids and Particulate Technologies, Faculty of Engineering, University of Wollongong, Wollongong, New South Wales, Australia. E-mail: david_hastie@uow.edu.au

Abstract

Seven belt conveyor trajectory methods, C.E.M.A., M.H.E.A., Booth, Golka, Korzen, Goodyear and Dunlop, are presented with their differences explained. Each method uses equations to determine the X and Y coordinates of the trajectory profile. Some methods also use graphical approaches which allow a quicker determination of the trajectory. Methods such as C.E.M.A., Goodyear and Dunlop use very few particle properties while the Korzen method uses many. The parameters used in each method have been investigated to evaluate the impact on the predicted conveyor trajectory. The parameters which showed the most influence are adhesive stress, coefficients of static and kinetic friction, particle shape and size, divergent coefficients.

Keywords: Trajectory, conveyor trajectory, conveyor belts, prediction models

Introduction

Accurate determination of conveyor trajectories is extremely important in the often complex design of conveyor transfers. Incorrect trajectory predictions can result in detrimental issues arising within a conveyor transfer, including; particle attrition, chute wear, dust generation, spillage, chute blockage and excessive noise. In transfer hood design, the impact angle of the incoming material stream should be kept low to minimise: loss of material velocity as it flows through the transfer; and impact and wear.

This study investigates aspects of the trajectory methods most widely referenced in the literature; C.E.M.A. (1966; 1979; 1994; 1997; 2005), M.H.E.A. (1986), Booth (1934), Golka et al. (2007), Korzen (1989), Goodyear (1975) and Dunlop (1982). These methods vary considerable with respect to the number of parameters used in the determination of the material trajectory, from the very basic to complex iterative approaches. This investigation includes altering values of the parameters exhibiting variability and determining the extent to which they influence the predicted trajectory. These trajectory methods are evaluated for both horizontal and inclined conveyors for a range of belt speeds and pulley diameters to evaluate both low-speed and high-speed conditions.

Variations of Trajectory Methods

There are various unique approaches to determining the material discharge trajectory from a conveyor head pulley, such as basic projectile motion principles (C.E.M.A., 1966; Goodyear, 1975; C.E.M.A., 1979; M.H.E.A., 1986; C.E.M.A., 1994; C.E.M.A., 1997; C.E.M.A., 2005), complex iterative solutions (Booth, 1934; Korzen, 1989), graphical methods (Booth, 1934;

Dunlop, 1982), one method including air drag (Korzen, 1989) and another incorporating divergent coefficients (Golka, 1992; Golka, 1993). It has been assumed that for all methods, the conveyor belt is loaded to full burden, for the determination of the upper trajectory stream, where applicable.

The methods employed to determine the discharge trajectory by C.E.M.A. (1966; 1979; 1994; 1997) and M.H.E.A. (1986) follow the same method, the difference being C.E.M.A. uses British units and M.H.E.A. uses metric. There are minor adjustments to some tabulated data for heights and fall distances specific to C.E.M.A. (1966; 1979; 1994; 1997). Both methods determine the trajectory based on the centroidal position of the material cross section and also allows for the upper and lower paths to be determined. For low-speed conveying, the discharge angle is determined from equation (1) and for a given conveyor geometry the only variable is belt speed. For high-speed conveying, the material discharges at the point of tangency between the belt and head pulley.

$$\alpha_d = \cos^{-1} \left[\frac{V_b^2 R_c}{g (R_p + b)^2} \right] \quad (1)$$

The trajectory can then be plotted for both low-speed and high-speed conveying by projecting a tangent line from the point where material leaves the head pulley. Time intervals are marked along this line then fall distances are projected vertically down from these points which are joined to produce the trajectory. C.E.M.A. (2005) has a slight modification to the way in which it determines the time interval along the tangency line for high-speed conditions, now based on the belt velocity not the tangential velocity.

Booth (1934) incorporated the angle at which material began to slip on the belt, α_r , with the view that this would aid in better accuracy. For high-speed conditions there is no material slip and the method used by C.E.M.A. and M.H.E.A. is applied using the drop heights supplied by Booth (1934). For low-speed conditions, an initial estimate of the discharge angle is found using equation (2) and the angle at which material slip first occurs on the belt, α_r , is determined by solving equation (3). The analysis by Booth produced equation (4), the constant of integration, C , which is determined using the initial conditions $V(\psi) = V_b$ and $\psi = \alpha_r$. Equations (2) and (4) can then be solved simultaneously with $V(\psi) = V_d$ and $\psi = \alpha_d$ to determine the discharge angle and discharge velocity. To produce low-speed trajectories, the method as for the high-speed condition is applied for the determined discharge angle.

$$\cos \alpha_d = \frac{V_b^2}{g R_b} \quad (2)$$

$$\cos \alpha_r - \frac{V_b^2}{g R_b} = \frac{1}{\mu_s} \sin \alpha_r \quad (3)$$

$$\frac{V^2(\psi)}{2 g R_b} = \frac{(2 \mu_s^2 - 1) \cos \psi - 3 \mu_s \sin \psi}{(4 \mu_s^2 + 1)} + C e^{2\mu_s \psi} \quad (4)$$

The coefficient of static friction between the material and conveyor belt used in equations (3) and (4) is the only parameter which is variable and will influence a given trajectory.

Golka (1992; 1993) used Cartesian coordinates to develop this trajectory. Two distinct discharge angles were developed, α_{d1} for the lower trajectory and α_{d2} for the upper trajectory, equations (5) and (6) respectively. Three individual cases were developed to accommodate low-speed and high-speed conditions and the transition between them (Table 1).

$$\alpha_{d1} = \cos^{-1} \left[\frac{V_1^2}{g R_p} \right] \quad (5)$$

$$\alpha_{d2} = \cos^{-1} \left[\frac{V_2^2}{g (R_p + h_d)} \right] \quad (6)$$

where,

$$V_2 = V_1 \left(1 + \frac{2h}{R_p} \right)^{0.5} \quad \text{and} \quad h_d = R_p \left(\left(1 + \frac{2h}{R_p} \right)^{0.5} - 1 \right)$$

Table 1 Discharge Angle Determination for the Golka (1992; 1993) Method

	CONDITION	α_{d1}	α_{d2}
CASE 1	$V_1 < V_{cr1}$ and $V_2 < V_{cr2}$	Equation (5)	Equation (6)
CASE 2	$V_1 > V_{cr1}$	Point of tangency	Point of tangency
CASE 3	$V_1 < V_{cr1}$ and $V_2 > V_{cr2}$	Equation (5)	Point of tangency

The use of the Cartesian coordinate system allows for the direct determination of the X and Y coordinates of the trajectory using selected time intervals. Golka (1992; 1993) includes two divergent coefficients, one for the lower trajectory and one for the upper trajectory, representing parameters such as air resistance, size distribution, permeability and particle segregation. These coefficients have been quantified by Golka et al. (2007), detailing the divergent coefficient ranges for specific conditions. Only belt speed, V_1 , will alter the discharge angle for the lower trajectory stream. The velocity, V_2 , and the height of material at discharge, h_d , will affect the upper trajectory stream.

Korzen (1989) employs a complex iterative approach to determine the material trajectory. This method addresses adhesive materials, inertia and material slip and uses static wall friction, μ_s , and kinetic wall friction, μ_k . The angle at which material first slips on the belt under low-speed conditions is determined from equation (7), with numerous variables which could alter the

trajectory path, including, static friction, adhesive stress, and specific gravity, explained further in the following sections.

$$\alpha_r = \tan^{-1} \mu_s \pm \sin^{-1} \left[\sin \left(\tan^{-1} \mu_s \right) \cdot \left(\frac{V_b^2}{R_c g} - 2 \frac{\sigma_a}{\gamma h} \right) \right] \quad (7)$$

The slip angle is required to evaluate the constant of integration, C, in equation (8), using the initial conditions $V(\psi) = V_b$ and $\psi = \alpha_r$. To determine the discharge angle, the conditions $V^2(\psi) = R_c g \cos \psi$ and $\psi = \alpha_d$ are used in equation (8).

$$V^2(\psi) = 2gR_c \left[\frac{(4\mu_k^2 - 1) \cos \psi - 5\mu_k \sin \psi}{(1 + 16\mu_k^2)} \right] + C e^{4\mu_k \psi} \quad (8)$$

The iterative solution is used when air drag effects are being considered and continued until an error of approximately 1% is reached for subsequent steps. The process ultimately determines the Y coordinate, resultant velocity and resultant angle for a given X coordinate. Korzen (1989) states that if particles have a mass greater than 1g, air drag effects can be neglected. If air drag is neglected, only the first step of the iterative process is performed.

Goodyear (1975) uses projectile motion equations to determine the trajectory path, shown in equations (9) and (10). As with previous methods, high-speed conveying results in material discharge at the point of tangency and low-speed conveying requires the calculation of the discharge angle as in equation (2) except using R_c instead of R_b .

$$X = V_b t \quad (9)$$

$$Y = \frac{1}{2} g t^2 \quad (10)$$

From the discharge point, a tangent line is drawn, along which multiple X coordinates based on equation (9), are placed. The corresponding Y coordinates represent the drop heights from each of these X points and when joined produce the trajectory. Other than belt speed, there are no parameters which can be altered to produce different trajectories.

Dunlop (1982) uses a graphical method to determine the trajectory for low-speed conditions. Knowing the belt speed and the head pulley diameter, the discharge angle and the incremental X distance along the tangent line can be obtained. The drop heights are calculated using equation (10). There are limitations to using the low-speed method, the chart only has pulley diameters in the range of 312 mm to 1,600 mm. For the high-speed condition, the X and Y coordinates of the trajectory are determined using equations (9) and (10) and are plotted from the tangent line drawn from the point of tangency. As with the Goodyear (1975) method, there are no variable parameters other than belt speed.

Trajectory Profiles

Direct trajectory comparisons using common parameters

Comparisons of the trajectory profiles for each method have been produced using the parameters in Table 2. Three belt speeds ($V_b = 1.25 \text{ ms}^{-1}$, 3.0 ms^{-1} and 6.0 ms^{-1}) and three pulley diameters ($D_p = 0.5 \text{ m}$, 1.0 m and 1.5 m) and the focus will be on horizontal conveyors, however the influence of varying the belt inclination angle will be discussed. Trajectories from declined

conveyors are only provided by three methods, C.E.M.A. (1966; 1979; 1994; 1997; 2005), M.H.E.A. (1986) and Goodyear (1975), so have not been included in these comparisons.

Table 2 Parameters Used in Trajectory Comparisons

Belt width	0.762	m
Belt thickness	0.01	m
Belt speed	1.5	ms ⁻¹
Pulley diameter	1	m
Belt inclination angle	0	°
Adhesive stress	0	kPa
Divergent coefficient, lower	0.1	
Divergent coefficient, upper	-0.1	
Coefficient of static friction	0.5	
Coefficient of kinetic friction	0.4	
Equivalent spherical particle diameter	0.001	m
Air viscosity	1.8x10 ⁻⁵	N s m ⁻²
Product density	2000	kg m ⁻³

The data in Table 2 has been used to produce low-speed trajectories for all presented methods, shown in Figure 1. It is evident that at this low belt speed there are two distinct groupings of methods. Subsequent analysis of other low-speed conveying showed that as the belt speed increased, the methods merged into one larger grouping as the angle of wrap decreased. As vertical displacement of the trajectories increases, the variation in the predicted trajectory profiles becomes more evident. It was also observed that the relative complexities of the Booth (1934) and Dunlop (1982) methods, still produced nearly identical trajectories.

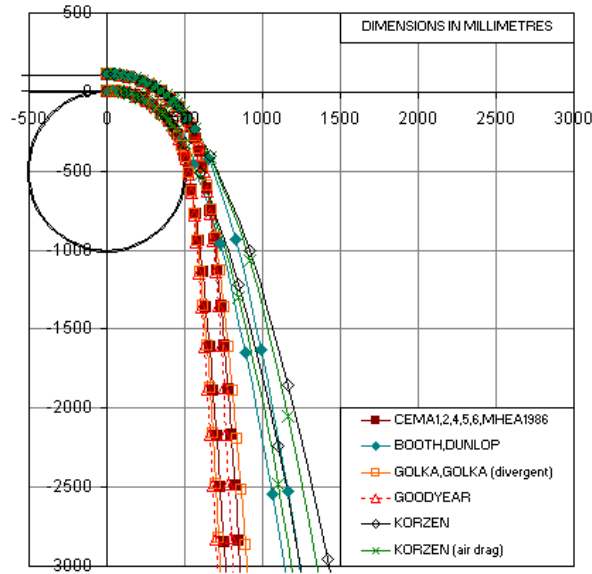


Figure 1 Low-Speed Horizontal Conveyor, Lower and Upper Trajectory Path,

Pulley Diameter, $D_p = 1.0$ m, Belt Velocity, $V_b = 1.25$ ms^{-1}

In order to investigate the effect of belt speed, two high-speed belt conditions have been selected, $V_b = 3.0$ ms^{-1} and $V_b = 6.0$ ms^{-1} . In Figures 2 and 3, the inclusion of air drag by Korzen (1989) results in a trajectory prediction much shallower than all other methods. When air drag is neglected, the resulting trajectory is located amongst the other methods.

Golka (1992; 1993) uses divergent coefficients to obtain a better approximation of the trajectory path. If the divergent coefficients are neglected, the resulting trajectories are identical to the Korzen (1989) method when air drag is neglected, as the equations are identical. For the $V_b = 3$ ms^{-1} and 6 ms^{-1} high-speed cases shown in Figures 2 and 3, the earlier C.E.M.A. (1966; 1979; 1994; 1997) methods and M.H.E.A. (1986) method generate the largest trajectory curve and as the discharge velocity increases, the variation from the other curves becomes more pronounced.

As with the low-speed conditions, the Booth (1934) and Dunlop (1982) methods again produce near identical trajectories.

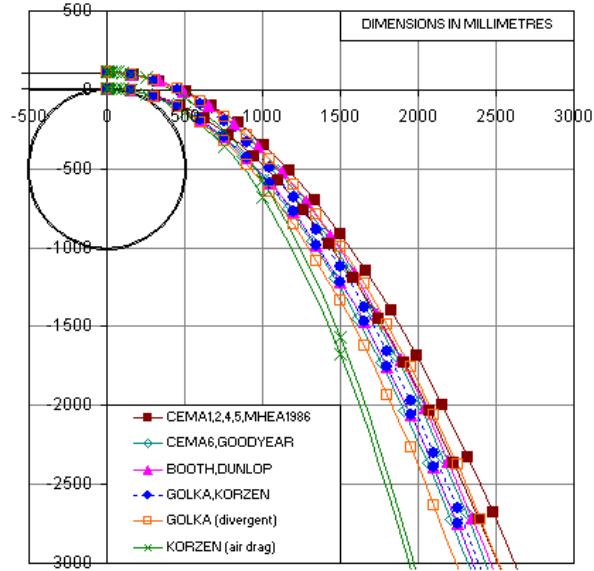


Figure 2 High-Speed Horizontal Conveyor, Lower and Upper Trajectory Path,

Pulley Diameter, $D_p = 1.0$ m, Belt Velocity, $V_b = 3.0 \text{ ms}^{-1}$

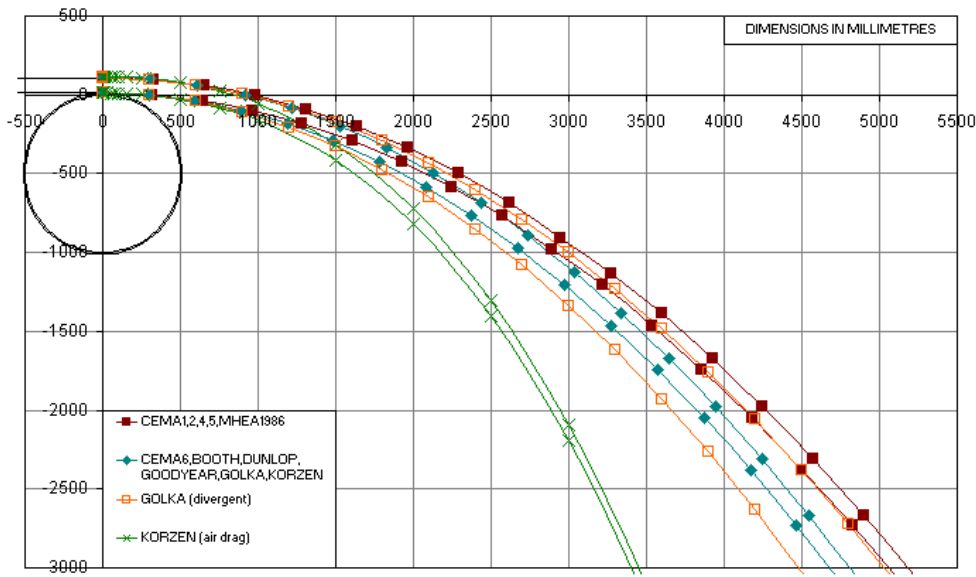


Figure 3 High-Speed Horizontal Conveyor, Lower and Upper Trajectory Path,

Pulley Diameter, $D_p = 1.0 \text{ m}$, Belt Velocity, $V_b = 6.0 \text{ ms}^{-1}$

Effect of belt inclination angle on trajectory profile

Of the seven trajectory methods, it was found that there were five unique equations used to determine the critical angle where the transition from low-speed to high-speed conveying conditions occurred. For the three pulley diameters selected, the variation in critical belt speed has been quantified and presented in Figure 4. As belt inclination increases, a lower belt speed sees the transition from low-speed to high-speed conveying. For high-speed conditions, the trajectory will be angled upward and the trajectory will commence before the vertical axis is reached. Figure 4 shows a sharp change in critical belt speed for the Dunlop method. These curves have been generated by extracting data directly from the chart provided by this method.

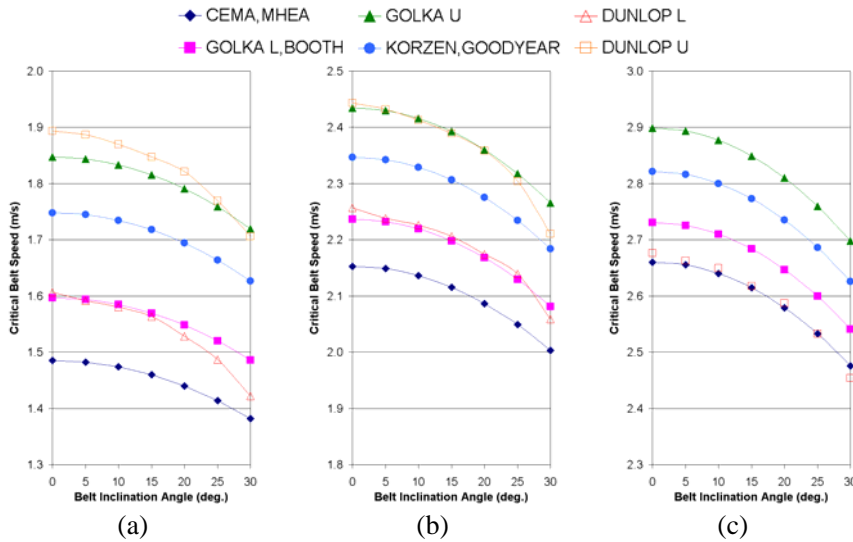


Figure 4 Critical Belt Speed Versus Belt Inclination Angle for Varying Pulley Diameters

(a) $D_p = 0.5$ m, (b) $D_p = 1.0$ m and (c) $D_p = 1.5$ m

Effect of modifying static and kinetic wall friction on trajectory profile

Static wall friction, μ_s , exists up to the point where slippage occurs and kinetic wall friction, μ_k , exists once motion commences and it is generally accepted that $\mu_k < \mu_s$ (Meriam and Kraige, 1987). The static wall friction has been varied in the Booth method (1934) between the values 0.1 and 0.9 and along with the parameters of Table 2, nine trajectories have been produced, as displayed in Figure 5. For the Korzen method (1989), both μ_s and μ_k are used. To investigate the effect of μ_s and μ_k on the trajectories, 36 individual trajectories were produced with μ_s ranging from 0.2 to 0.9 and μ_k ranging from 0.1 to 0.8, the results shown in Figure 6. For low-speed conditions, a band of trajectories results as frictions vary whereas for high-speed conditions only one unique trajectory is produced. This is due to the coefficient of static and kinetic wall friction only being used in the determination of low-speed discharge angles.

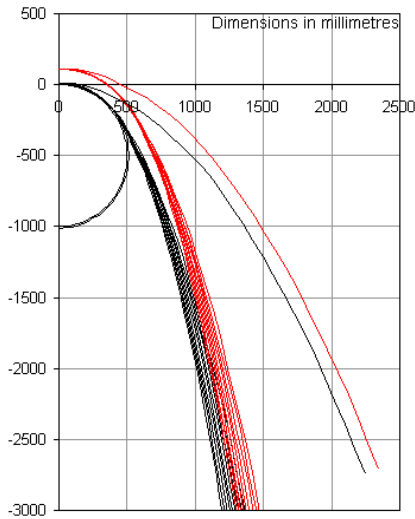


Figure 5 Booth method showing belt speeds

$$V_b = 1.5 \text{ ms}^{-1} \text{ and } V_b = 3 \text{ ms}^{-1}$$

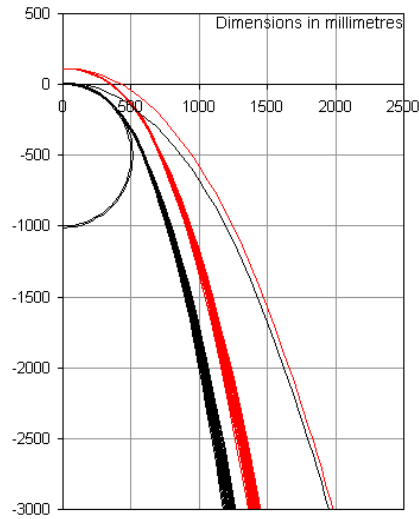


Figure 6 Korzen method showing belt speeds

$$V_b = 1.5 \text{ ms}^{-1} \text{ and } V_b = 3 \text{ ms}^{-1}$$

Effect of divergent coefficients on trajectory profile

Originally Golka (1992; 1993) gave no explanation as to how the divergent coefficients were quantified. More recently, Golka et al. (2007) presented a detailed table of the factors which define how the divergent coefficients are weighted. General rules to follow in defining the divergent coefficients are;

- dusty materials have a higher value than non-dusty materials,
- larger particle sizes have a lower value than fine particles,
- low belt speed results in lower values to the high belt speed equivalents.

Illustrating the effect of this parameter, divergent coefficient values ranging from 0 to ± 0.2 have been applied to the parameters of Table 2 with a belt speed on 3 ms^{-1} to produce trajectories. Divergent coefficients of ± 0.1 correspond to a non-dusty material with lump size in excess of

200 mm while divergent coefficients of ± 0.2 correspond to a very dusty material with a maximum particle diameter of 3 mm. Figure 7 displays the results and as a comparison, the case of no divergent coefficients has been added.

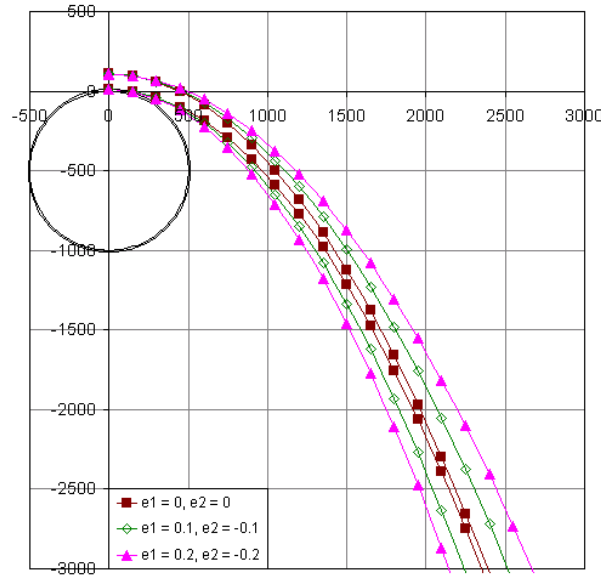


Figure 7 Variation in Trajectories Based on Different Divergent Coefficients (Golka et al., 2007)

Effect of particle shape and size on trajectory profile

The Korzen (1989) trajectory method includes the equivalent spherical particle diameter, d_k , and has been investigated to determine the effect that this parameter has on determining the resulting conveyor trajectory. Using the particle sizes shown in Table 4 and the parameters from Table 2, the trajectories shown in Figure 8 (a), (b) and (c) have been produced. Each figure includes the no air drag condition for comparison. The results show that as particle mass increases, the trajectory converges to that of the no air drag condition. This corresponds with the claim by Korzen (1989) that air drag can be neglected for particles over 1g in mass.

Table 4 Selected Equivalent Spherical Particle Diameters for Comparison

d_k (mm)	Unit mass of particle (g)
0.5	0.0001
1	0.001
10	1.05

In reality a particle size distribution (PSD) would exist, creating a degree of segregation within the particle stream. This would result in the fines behaving as shown in Figure 8(a) while the courser material would behave more like that shown in Figure 8(c).

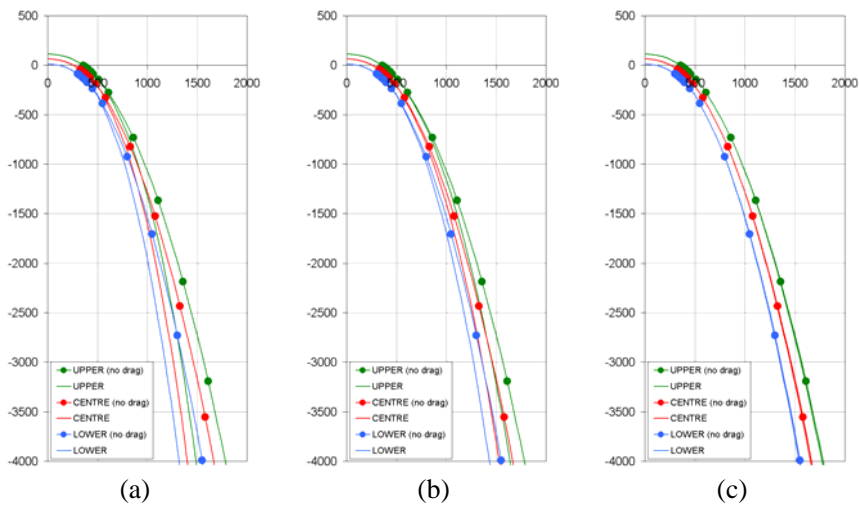


Figure 8 Effect of particle shape and size for (a) $d_k = 0.5$ mm, $d_m = 0.0001$ g,

(b) $d_k = 1.0$ mm, $d_m = 0.001$ g and (c) $d_k = 10$ mm, $d_m = 1.05$ g

Effect of adhesive stress on trajectory profile

There is an adhesive stress component in equation (7) of the Korzen method (1989). In the case of all the comparisons presented above, the adhesive stress has been set to zero to keep comparisons consistent against other methods. To illustrate the effect of varying the adhesive stress, a pulley diameter of $D_p = 1.0$ m was selected along with a range of adhesive stresses from 0 kPa to 2.5 kPa and applied, see Figure 9.

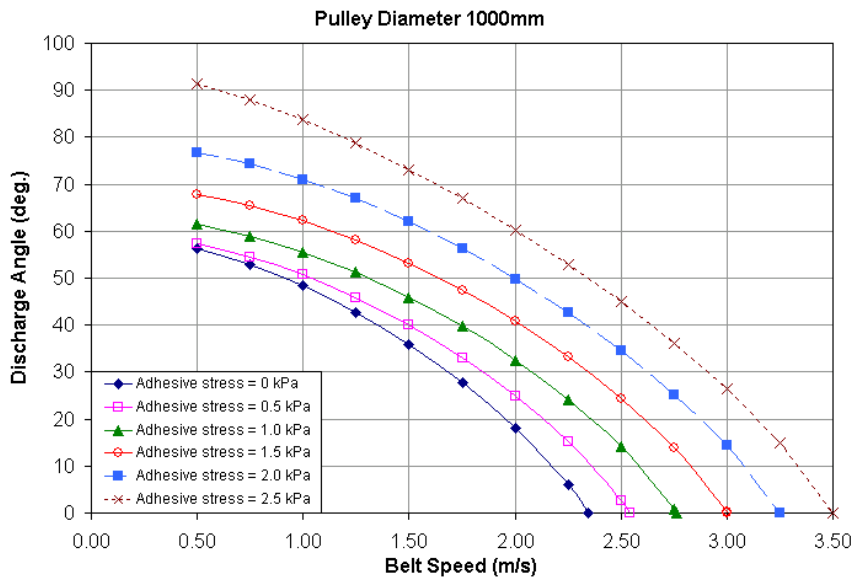


Figure 9 Effect of adhesive stress on discharge angle in the Korzen (1989) method

As adhesive stress increases for a given belt speed, so too the discharge angle increases. For these comparisons, an adhesive stress of 2.5 kPa results in a discharge angle of 91.3° for a belt speed of 0.5 ms^{-1} . This implies that material will not discharge until it passes the most horizontal point on the head pulley and would be in actual fact be discharging under the conveyor. Further increase of the adhesive stress results in no solution being possible when solving equation (7).

Effect of bulk density on trajectory profile

The Korzen method (1989) is the only one to incorporate material bulk density. The bulk density only influences the conveyor trajectory when air drag effects are considered and comparisons have been made using the parameters presented in Table 2 while only varying bulk density. Figure 10 presents four sets of trajectory curves, the set with the largest trajectory represents the case when air drag has been neglected from the calculations. The three remaining sets of trajectories show that as bulk density increases, the trajectory streams project further and in theory, given a high enough bulk density, the trajectory will converge on that of the no air drag condition.

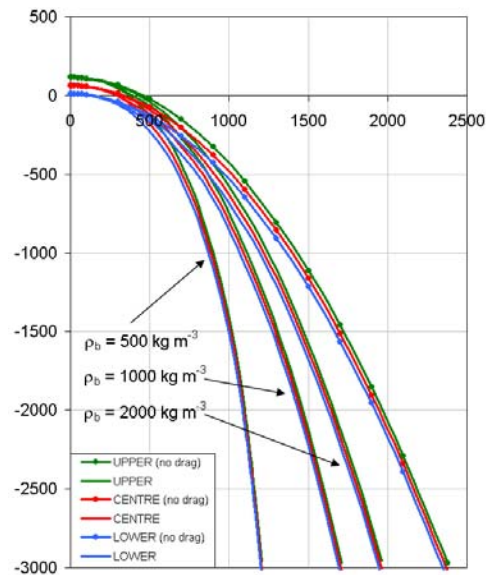


Figure 10 Effect of bulk density on trajectory profile

Conclusion

This paper has reviewed the more widely used and/or readily available trajectory prediction methods available in the literature. The differing complexities of these methods results in a range of influences contributing to the final trajectory. The methods of C.E.M.A. (1966; 1979; 1994; 1997; 2005) and M.H.E.A. (1986) do not rely on particle characteristics. Golka (1992; 1993) did not originally detail the method of obtaining the divergent coefficients but has in more recent work (Golka et al., 2007). Varying these divergent coefficients shows that there are noticeable differences to the trajectory profile dependent on the particle size, dustiness of the material and also belt speed. Korzen (1989) uses the most parameters which can potentially influence the final trajectory profile. Static and kinetic wall friction, particle shape and size, adhesive stress and bulk density have all been shown to affect the resulting trajectory profiles.

The incorporation of air drag in the trajectory predictions causes a substantial variation from the other trajectory methods. Whether this is truly representative of an actual trajectory needs to be explored further.

The differing approaches to determine trajectories results in some significant differences, which cannot all be correct. With the commissioning of a unique conveyor transfer research facility at the University of Wollongong, it is the intention to test a number of materials with varying particle size, shape and density to validate the trajectory methods.

Acknowledgments

The authors wish to acknowledge the support of the Australian Research Council, Rio Tinto Technology and Innovation and Rio Tinto Iron Ore Expansion Projects for their financial and in-kind contributions to the Linkage Project which allows this research to be pursued.

List of Symbols

b	belt thickness, m
C	constant of integration, -
d_k	equivalent spherical particle diameter, m
dm	mass of particle, g
g	gravity, $m\ s^{-2}$
h	material height, m
h_d	height of material stream at discharge, m
R_b	belt radius, m
R_c	radius to centre/centroid of material stream, m
R_p	head pulley radius, m
V_1	velocity of lower stream, ms^{-1}
V_2	velocity of upper stream, ms^{-1}
V_b	belt velocity, ms^{-1}
V_{cr1}	critical velocity for lower trajectory, ms^{-1}
V_{cr2}	critical velocity for upper trajectory, ms^{-1}
V_d	discharge velocity, ms^{-1}
α_d	discharge angle, $^\circ$

α_{d1}	discharge angle for the lower trajectory, °
α_{d2}	discharge angle for the upper trajectory, °
α_r	angle where material begins to slip on the belt, °
γ	specific gravity of material, kN m^{-3}
μ_k	kinetic coefficient of wall friction, -
μ_s	static coefficient of wall friction, -
σ_a	adhesive stress, kN m^{-2}
ψ	arbitrary angle, °

References

- Booth, E. P. O. (1934). "*Trajectories from Conveyors - Method of Calculating Them Corrected*". Engineering and Mining Journal, Vol. 135, No. 12, December, pp. 552 - 554.
- C.E.M.A. (1966). *Belt Conveyors for Bulk Materials*. 1st Ed, Conveyor Equipment Manufacturers Association. pp. 332.
- C.E.M.A. (1979). *Belt Conveyors for Bulk Materials*. 2nd Ed, Conveyor Equipment Manufacturers Association. pp. 346.
- C.E.M.A. (1994). *Belt Conveyors for Bulk Materials*. 4th Ed, Conveyor Equipment Manufacturers Association. pp. 374.
- C.E.M.A. (1997). *Belt Conveyors for Bulk Materials*. 5th Ed, Conveyor Equipment Manufacturers Association. pp. 430.
- C.E.M.A. (2005). *Belt Conveyors for Bulk Materials*. 6th Ed, Conveyor Equipment Manufacturers Association. pp. 599.
- Dunlop (1982). "*Dunlop Industrial Conveyor Manual*", Dunlop Industrial, pp. 9.1 – 9.5.
- Golka, K. (1992). "*Discharge Trajectories of Bulk Solids*". 4th International Conference on Bulk Materials Storage, Handling and Transportation, Wollongong, NSW, Australia, 6th - 8th July, pp. 497 - 503.

Golka, K. (1993). "*Prediction of the Discharge Trajectories of Bulk Materials*". Bulk Solids Handling, Vol. 13, No. 4, November, pp. 763 - 766.

Golka, K., Bolliger, G. and Vasili, C. (2007). *Belt Conveyors Principles for Calculation and Design*. Lugarno, N.S.W., Australia, K. Golka, G. Bolliger, C. Vasili. pp. 288.

Formatted: German
(Germany)

Goodyear (1975). "*Goodyear Handbook of Conveyor & Elevator Belting*", pp. Section 11.

Korzen, Z. (1989). "*Mechanics of Belt Conveyor Discharge Process as Affected by Air Drag*". Bulk Solids Handling, Vol. 9, No. 3, August, pp. 289 - 297.

M.H.E.A. (1986). *Recommended Practice for Troughed Belt Conveyors*, Mechanical Handling Engineer's Association. pp. 199.

Meriam, J. L. and Kraige, L. G. (1987). *Engineering Mechanics - Statics*. 2nd Ed, John Wiley and Sons. pp. 454.